Int J Adv Eng Sci Appl Math (July–December 2014) 6(3–4):183–194
DOI 10.1007/s12572-015-0117-2

Mathematical modelling of a cryogenic engine

V. Narayanan · M. S. Suresh · N. Jayan · K. S. Bijukumar

Published online: 10 February 2015
© Indian Institute of Technology Madras 2015

Abstract Cryogenic propulsion systems using liquid hydrogen and liquid oxygen propellant combination are used in satellite launch vehicles in view of the higher specific impulse (I_{SP}). Due to extreme low temperature of cryogenic propellant and low density and explosive nature of LH_2, the development of cryogenic propulsion system is very complex and time consuming. In ISRO an indigenous cryogenic upper stage powered by an engine developing a nominal thrust of 73.5 kN in vacuum with a propellant loading of 12.8 tonnes is developed and successfully flight tested for the first time in GSLV D5 flight on 5th January 2014. A mathematical model is developed for finalizing the engine start and shut off sequence, ensuring smooth and safe ignition, predicting performance of subsystems under transient phase, nominal and off nominal conditions, control systems parameter settings and for the performance estimation of engine in sea level and flight. This paper highlights the configuration and working of a cryogenic engine, mathematical modelling of the engine, applications of the model in the cryogenic engine development and comparison of predicted values with the test results.

Keywords Cryogenic engine · Mathematical model · Transient build up · Engine performance

V. Narayanan
Cryogenic Propulsion and Stage Entity, ISRO,
Thiruvananthapuram, Kerela, India
e-mail: v_narayanan@lpsc.gov.in

M. S. Suresh
Cryogenic Propulsion Engines Group/ISRO, ISRO,
Thiruvananthapuram, Kerela, India
e-mail: ms_suresh@lpsc.gov.in

N. Jayan · K. S. Bijukumar (✉)
Engine Fluid System and Analysis Division/ISRO, ISRO,
Thiruvananthapuram, Kerela, India
e-mail: ks_bijukumar@lpsc.gov.in

N. Jayan
e-mail: n_jayan@lpsc.gov.in

List of symbols

Pressure

P_C	Main engine chamber pressure
PGGE	Gas generator chamber pressure
PFPI	Pressure at main fuel pump inlet
PHPD	Pressure at main fuel pump delivery
POPI	Pressure at main oxidizer pump inlet
POPD	Pressure at main oxidizer pump delivery
PHCHE	Pressure of hydrogen at coolant channel exit
POME	Pressure of LOX at the exit of mixture ratio controller
PGTE	Pressure at the exit of main turbine
POAE	Pressure of LOX at the exit of absolute velocity regulator
PHBTI	Pressure at hydrogen booster turbine inlet
PHBTD	Pressure at hydrogen booster turbine exit
PFBO	Pressure at fuel booster pump outlet
POBTI	Pressure at oxygen booster turbine inlet
POBO	Pressure at oxygen booster pump outlet

Temperature

TFPI	Fluid temperature at main fuel pump inlet
TOPI	Fluid temperature at main oxidizer pump inlet
TOPD	Fluid temperature at main oxidizer pump delivery
THCHE	Fluid temperature of hydrogen at coolant channel exit

THBTD Fluid temperature at hydrogen booster turbine exit

Flow rate

m_{lox} LOX flow rate
m_f Hydrogen flow rate
ME Main engine
GG Gas generator
OBT Oxidizer booster turbine
FBT Fuel booster turbine
SE Steering engine
MOP Main oxidizer pump
V, U Velocity
f Friction factor, body force
L Length
A_t Throat area
A Turbine nozzle area
C* Characteristic velocity
hg Gas side convective heat transfer coefficient
hc Coolant side heat transfer coefficient
qc Heat flux due to convection
qr Heat flux due to radiation
q Combined heat flux
k Conductivity of the material
t Shell thikness
ηf Fin effectiveness
H Total enthalpy
C Concentration
τ Shear stress
μ Viscocity
ρ Density
P Pressure
Q, R Source terms
h Static enthalpy
E Total energy
e Internal energy
J Diffusion flux

1 Introduction

Cryogenic propulsion systems using liquid hydrogen and liquid oxygen propellant combination are used in satellite launch vehicles in view of the higher specific impulse (I_{SP}). The specific impulse of cryogenic propulsion is 450–460 s as compared with 260–275 s of solid propulsion, 280–315 s of earth storable liquid propulsion and 300–350 s of semi-cryogenic propulsion systems. Due to extreme low temperature of cryogenic propellants and low density & explosive nature of LH_2, the development of cryogenic propulsion system is very complex and time consuming. In India, to meet the initial requirements of GSLV MkII vehicle, seven cryogenic stages (CS) were procured from Russia and for the continued self reliant operation of the vehicle, indigenous cryogenic upper stage (CUS) powered by an engine developing a nominal thrust of 73.5 kN in vacuum with a propellant loading of 12.8 tonnes is developed. Mathematical modelling of engine plays a crucial role in the development of a cryogenic engine. It helps for finalizing the engine start and shut off sequence, ensuring smooth and safe ignition, predicting performance of subsystems during transient, steady state and off nominal conditions, control systems parameter settings and for the performance estimation of engine in flight. A mathematical model is developed for the CUS engine and extensively used during the engine development and performance prediction of first flight engine. This paper highlights the configuration and working of a cryogenic engine, mathematical modelling of the engine, applications of the model in the cryogenic engine development and comparison of predicted values with the flight data.

2 Configuration of the engine

The CUS engine (Fig. 1) consists of a main engine and two steering engines capable of developing a nominal thrust of 73.5 kN in vacuum with a specific impulse of 454 s. It works on staged combustion cycle in which the entire gas generated in the pre-combustion chamber is fed into the main thrust chamber after driving the turbine, which eventually results in maximum performance. The main engine is regeneratively cooled and turbopump fed. It has a dump cooled nozzle extension with an area ratio 199. The steering engines employed for vehicle control has a regeneratively cooled nozzle with an area ratio of 57. The turbopump system consists of a main turbopump, fuel (LH_2) and oxidizer (LOX) booster turbopumps. The LOX and LH_2 booster turbopumps are mounted in the respective propellant tanks to provide sufficient pressure of propellant at the inlet of main pumps to ensure cavitation free operation. The main turbine is driven by the hot gas generated by the pre-burner which is also regeneratively cooled. The LH_2 booster turbine is driven by the gaseous hydrogen tapped from the coolant outlet manifold of main thrust chamber. The LOX booster turbine is driven by high pressure LOX tapped at the outlet of LOX main pump. LOX and LH_2 propellant combination being non- hypergolic, pyrogen igniters are used for the main engine, steering engines and pre burner to initiate combustion. High pressure GHe ($\sim$10.5 MPa) stored in a gas bottle is used for starting the H_2 booster turbo-pump and the main turbo-pump is started in expander mode. The engine has mixture ratio control (MRC) and thrust regulation systems to maintain the required mixture ratio and thrust level during its operation.

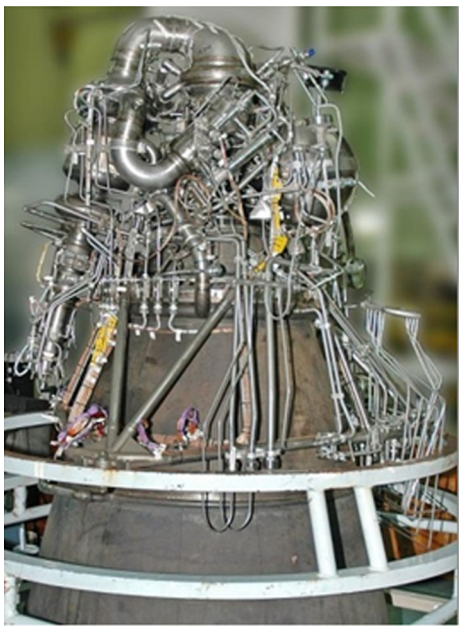

Fig. 1 Cryogenic engine

3 Scheme of engine operation

LOX at 78 K temperature and 0.17 MPa pressure is stored in the LOX tank. The LOX booster pump driven by a hydraulic impulse turbine raises the pressure sufficiently high to meet the net positive suction head (NPSH) requirement of the LOX main pump. The main pump increases the LOX pressure to the required level. The high pressure LOX from the main pump outlet gets divided into three streams. One portion drives the booster turbine and joins at the booster pump outlet. The second stream is regulated by the thrust regulator and fed to the gas generator. The third stream is regulated by the MRC and is injected into the main engine and steering engines. LH_2 at a temperature of 20.8 K and a pressure of 0.19 MPa is stored in the LH_2 tank. The LH_2 booster pump driven by a gas turbine raises the pressure to meet the NPSH requirement of the main pump. The main LH_2 pump raises the pressure to the required level and feed it to the main engine cooling channel jacket. LH_2 cools the Main engine up to an area ratio of 114 and gets collected in the hydrogen manifold. From the manifold hydrogen gets divided into six streams. The first and the major portion is fed into the pre-burner. The second and third streams are used as the regenerative coolant for the steering engines and are then injected into the respective steering engine chambers. The fourth stream is used for driving the fuel booster turbine and is vented out through two dump nozzles after cooling the main engine nozzle extension (from area ratio 114 to 199). The final portion is used for pressurizing the hydrogen tank. The combustion product from the pre-burner is used for driving the main turbine and is then injected into the main combustion chamber.

Before starting the engine the LOX and LH_2 feed systems are chilled down to the required temperatures and the thrust and mixture ratio regulators are brought to least area position which corresponds to about 50 % of the engine normal working condition. After completion of the chill down operation (time T0), high pressure helium gas stored in start up system gas bottle is admitted to drive the fuel booster turbine. The hydrogen valve is opened and LH_2 is admitted through the main engine cooling channels, gas generator and steering engines at T0 + 0.5 s. LH_2 gets evaporated and drives the main turbopump system in expander mode and in turn gets injected into the main engine. LOX from the tank flows through the booster pump to the main pump due to the pressure difference and LOX Main pump rotation. At T0 + 0.5 s the igniters of steering engine are switched ON and LOX is also admitted to the steering engines. At T0 + 0.9 s, main engine igniter is switched ON. At T0 + 1.4 s LOX is admitted to the main engine and pre burner igniter is switched ON. The main engine gets ignited at around T0 + 1.8 s. At T0 + 1.9 s LOX is admitted to the pre burner and the thrust and mixture ratio regulators are commanded to move to the nominal working position. The LOX line purging with GHe is stopped while admitting LOX to Steering engines, pre-burner and Main engine. Hot combustion gas from the pre-burner drives the main turbine after GG ignition which is at around T0 + 2.2 s. The engine reaches the nominal working mode between 5 to 7 s. The working of the engine in the nominal mode is checked between T0 + 9 to T0 + 10.5 s using the vehicle acceleration data. Once the engine starting and nominal functioning is ensured, the thrust and mixture ratio regulation systems are brought to the closed loop regulation mode at T0 + 11 s. At T0 + 20 s engine is up rated to 109.5 % thrust level and the engine is again throttled to nominal operating mode at 425 s and operated for another 295 s before shut down. Engine is shutdown by executing a set of commands sequentially. Fluid circuit diagram of CUS engine is shown in Fig. 2.

4 Mathematical modelling

Mathematical modeling of cryogenic propellant rocket engine system is typically based upon the assumption of approximating the engine as a series of homogenous control volumes. Within each volume the principles of conservation of mass and energy are applied. This includes the incorporation of thermal analysis, wherever appropriate, when temperature changes in the hardware itself are influencing the fluid conditions. Further, these volumes are

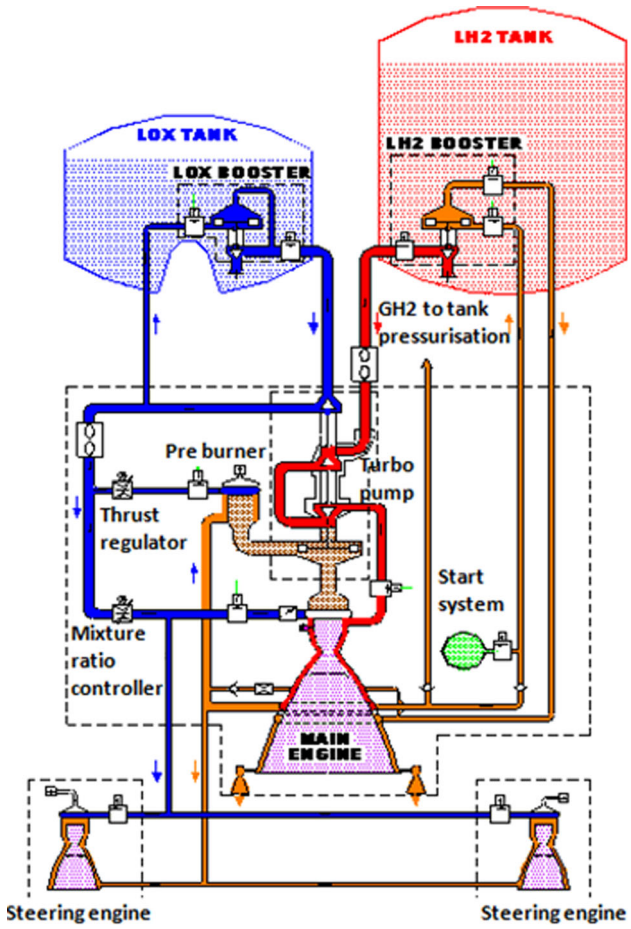

Fig. 2 Fluid circuit diagram for CUS engine

connected to create a fluid flow network to which the principle of the conservation of linear momentum is applied as a governing equation to determine the transport of fluid from one volume to another. Rotating machinery is included within the solution process via the use of the conservation of angular momentum. Combustion zones, inside the combustion devices, require the additional consideration of the addition of chemical energy into the system and the change in the energy content of the working fluids. For this CFD simulation along with combustion modeling is used. All of this together constitutes the complete system that must be accurately modeled through mathematical and computational analysis.

The CUS engine has mainly four phases of operation as shown in Fig. 3. The first phase is the expander mode of engine starting till ignition of GG followed by boot strap mode of build up to steady state conditions. Thereafter the engine will be controlled by the closed loop thrust and MR control system and the fourth phase is the shutdown transient phase. A quasi steady state mathematical model is developed using simultaneous solution method to predict the transient and control regimes of the engine. The expander mode build up zone is the most complex zone to be modeled because of the two phase flow conditions and the inertial characteristics of the turbo pump systems. This zone is modeled using sub system characteristic equations and coefficients for coolant channel characteristics and turbo pump head-flow and efficiency functions at low power levels corrected using cold start test results. Overall algorithm flowchart used for the model is given in Fig. 4. Figures 5 and 6 show the flowcharts used for the estimation of flow and pressure budgets of LH_2 and LOX feed systems respectively. Figure 7 gives the flowchart for the modelling of booster turbo pumps.

5 System equations

5.1 Gas orifice

Flow through the throat of the thrust chamber, injector elements, turbine nozzles etc. are approximated as the orifice flows and the governing equations used for this flow areFor unchoked condition

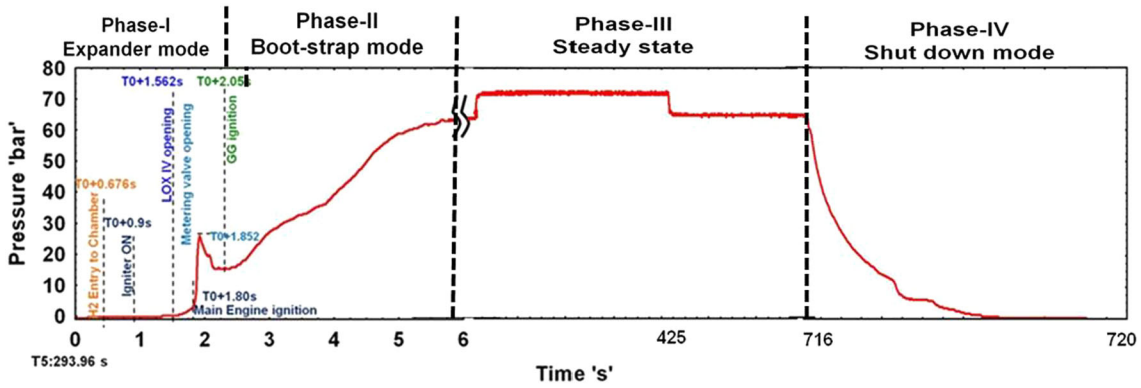

Fig. 3 Expander mode to boot strap mode transition

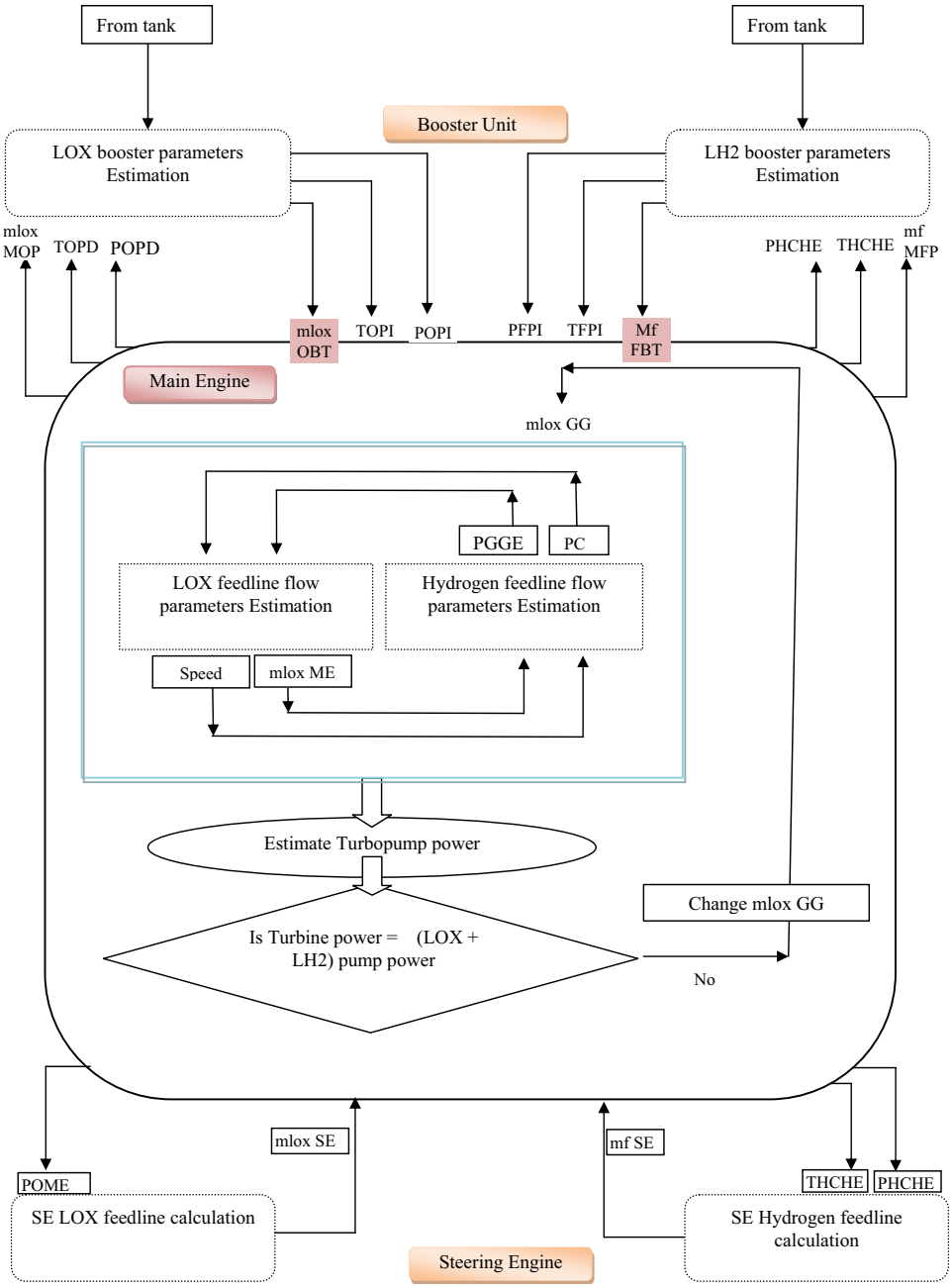

Fig. 4 Steady state algorithm flowchart

$$P_{inlet} = \frac{\dot{m}\sqrt{\frac{RT_{inlet}}{M}}}{C_d A\sqrt{\frac{2\gamma}{\gamma-1}\left[\left(\frac{P_{exit}}{P_{inlet}}\right)^{\frac{2}{\gamma}} - \left(\frac{P_{exit}}{P_{inlet}}\right)^{\frac{\gamma+1}{\gamma}}\right]}} \quad (1)$$

For choked condition

$$P_{inlet} = \frac{\dot{m}\sqrt{\frac{RT_{inlet}}{M}}}{C_d A\sqrt{\gamma\left(\frac{2}{\gamma+1}\right)^{\frac{(\gamma+1)}{\gamma}}}} \quad (2)$$

6 Combustion chamber

Chamber pressure developed in the combustion chamber is estimated using the equation [1]

$$P_c = \frac{\dot{m}_t x C^*}{A_t} \quad (3)$$

$$C^* = f(MR, P_c)$$

$$\dot{m}_t = \dot{m}_{LOX} + \dot{m}_{H_2}$$

$$MR = \frac{\dot{m}_{LOX}}{\dot{m}_{H_2}} \quad (4)$$

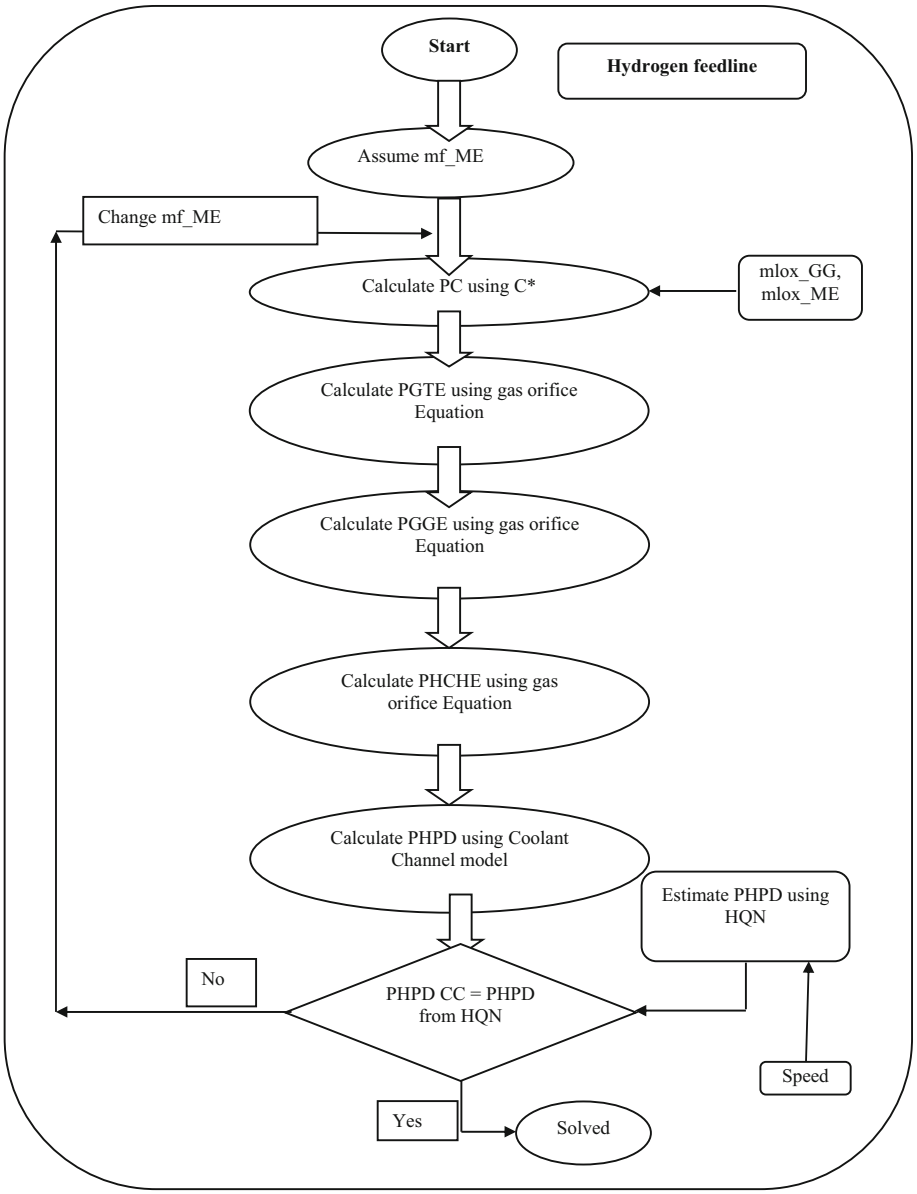

Fig. 5 Flowchart for hydrogen feedline

6.1 Pre burner

Chamber pressure in the pre burner is estimated using the equation

$$P_c = \frac{\dot{m}_t x C^*}{A_t} \tag{5}$$

7 Coolant channel

The pressure drop in the coolant channel is estimated using the following set of equations for gas flow:

Transient phase

$$\frac{\Delta P}{\left(\frac{\dot{m}^2}{\rho}\right)} = cons\tan t \tag{6}$$

Further the density is assumed to be proportional to ratio of average pressure and average temperature across the coolant channel. i.e.

$$\frac{\Delta P}{\dot{m}^2}\frac{P_{avg}}{T_{avg}} = cons\tan t. \tag{7}$$

As the two phase flow is involved during transient, this model will not be valid directly. Hence it is assumed that

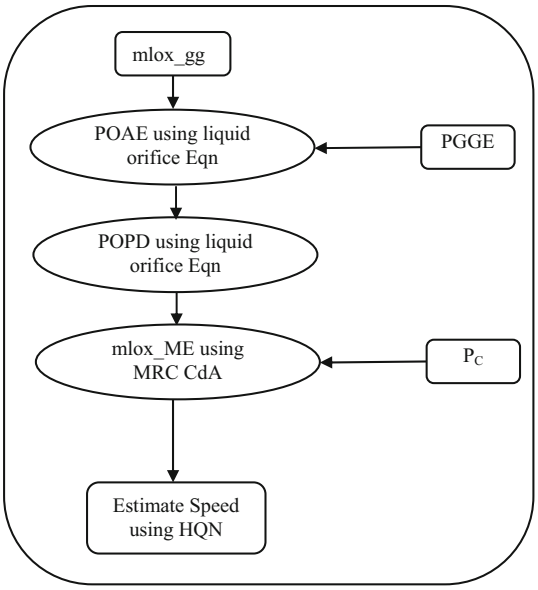

Fig. 6 Flowchart for LOX feedline

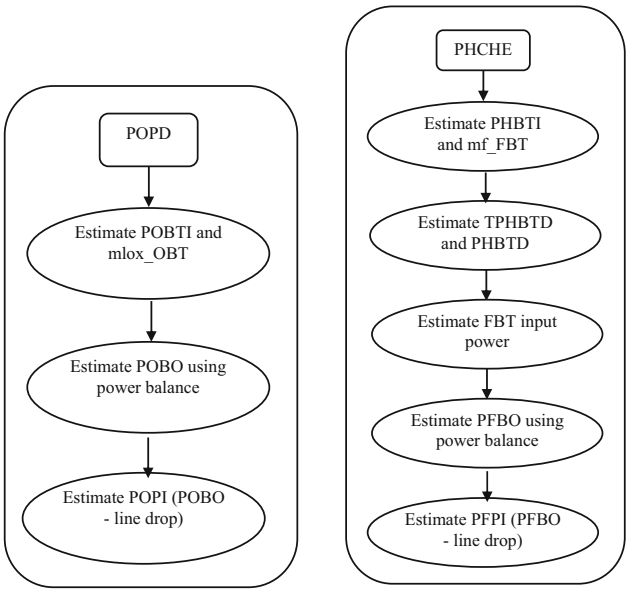
POPD
Estimate POBTI and mlox_OBT
Estimate POBO using power balance
Estimate POPI (POBO - line drop)
PHCHE
Estimate PHBTI and mf_FBT
Estimate TPHBTD and PHBTD
Estimate FBT input power
Estimate PFBO using power balance
Estimate PFPI (PFBO - line drop)

Fig. 7 Flowchart for booster turbo pumps

the constant will now have a varying factor with respect to mass flow rate.

$$\frac{\Delta P}{\dot{m}^2}\frac{P_{avg}}{T_{avg}} = K \times k(\dot{m}). \tag{8}$$

Steady state regime During the steady state regime coolant channel pressure drop is estimated using forward marching method. The one dimensional steady state heat transfer equations used are as follows:Heat transfer from hot gas to the chamber wall,

$$q = q_c + q_r \tag{9}$$

$$q_c = h_g \times \left(T_{aw} - T_{wg}\right) \tag{10}$$

heat transfer through the chamber wall is $q = (k/t) \times \left(T_{wg} - T_{wc}\right)$ and the heat transfer from chamber wall to coolant is

$$q = \eta_f h_c (T_{wc} - T_{co}) \tag{11}$$

For the calculation of gas side heat transfer co-efficient (hg), the modified Bartz's equation [2] given below has been used in this study

$$h_g = \frac{0.026}{D_t^{0.2}}\left[\frac{\mu_g^{0.2} Cp_g}{\mathrm{Pr}_g^{0.6}}\right]\left[\frac{P_c g}{C^*_{Design}}\right]^{0.8}\left[\frac{D_t}{R_c}\right]^{0.1}\left[\frac{A_t}{A}\right]^{0.9}\sigma$$

where

$$\sigma = \left[0.5\frac{T_{wg}}{T_{cth}}\left(1 + \frac{(\gamma-1)M^2}{2}\right) + 0.5\right]^{-0.68} \times \left[1 + \frac{(\gamma-1)}{2}M^2\right]^{-0.12} \tag{12}$$

The specific heat (Cpg), the viscosity (μg) and Prandtl No. (Prg) of gas has been calculated for chamber conditions by using the following equation.

$$C_{pg} = \gamma R/(\gamma - 1)$$

$$P_{rg} = 4\gamma/(9\gamma - 5)$$

$$\mu_g = 46.6 \times 10^{-10}(\mathrm{Mol.wt})^{0.5}\mathrm{T_g^{0.6}}$$

The combustion gas temperature (Tcth). Mach number (M) and gamma (γ) for the local points has been obtained from the NASA-SP-273 program [3].

The adiabatic wall temperature at different location is calculated from the local gas temperature (Tcth) considering a stagnation recovery factor—Rf.

The heat flux due to radiation of the combustion gases to the copper inner shell is found out using the relation:

$$q_r = \varepsilon_c.\varepsilon_g\sigma\left(T_g\right)^4 \tag{13}$$

where Tg is the hot gas temperature. σis the Stefan–Boltzman and ε_c and ε_g are the emmissitivities of chamber material and the combustion products.

$$R_f = \frac{1 + p_r^{0.33}\left(1 + \frac{(\gamma-1)}{2}M^2\right)}{\left(1 + \frac{(\gamma-1)}{2}M^2\right)} \tag{14}$$

The coolant side heat transfer co-effiecient (hc) is obtained the Sieder Tate's equation as given below

$$hc = 0.029\left[\frac{C_{pc}\mu_c^{0.2}}{P_{rc}^{0.66}}\right]\left[\frac{G^{0.8}}{D_h^{0.2}}\right]\left[\frac{T_{co}}{T_{wc}}\right]^{0.55} \tag{15}$$

where Cpc, μc and Prc are the specific heat at constant pressure, viscosity and the Prandtl number of the coolant at that coolant temperature. G is the mass flux of the coolant and dh is the hydraulic diameter of the coolant passage.

To consider the augmented heat transfer through the rib into the channel, a fin effectiveness given by

$$E_f = \frac{w}{(w + r_w)} + \frac{2d}{(w + r_w)} \left[\frac{\tanh\left[\sqrt{\frac{2h_c r_w}{k}} \frac{d}{r_w} \right]}{\sqrt{\frac{2h_c r_w}{k}} \frac{d}{r_w}} \right] \tag{16}$$

where w, rw and d are the channel width, rib width and depth of the cooling channel.

The coolant pressure drop at each of the computing stations while marching forward in space is computed as $\Delta p = (f\ \Delta l\ v^2 \rho) / (2\ g\ d_h)$ where v is the local coolant velocity, ρis the density, d_h is the hydraulic diameter and Δl is the length of the coolant element considered. The friction factor f is obtained iteratively as a function of coolant Reynolds number and roughness protrusion height, using the Colebrooke equation

$$\frac{1}{\sqrt{f}} = 1.74 - 2\log_{10}\left[\left(\frac{2e}{d_h} \right) + \frac{18.7}{\mathrm{Re}\sqrt{f}} \right] \tag{17}$$

where e is the roughness protrusion height, dh is the hydraulic diameter and Re is Reynolds number.

8 Turbo-pump

8.1 Pump

Volume flow rate and head of the pump are given by

$$Q = \frac{\dot{m}}{\rho}$$

$$\Delta H = \frac{P_{exit}}{\rho_{exit} g} - \frac{P_{inlet}}{\rho_{inlet} g} \tag{18}$$

HQN characteristics equation of the pump is

$$\frac{\Delta H}{N^2} = c_1 + c_2 \left(\frac{Q}{N} \right) + c_3 \left(\frac{Q}{N} \right)^2 \tag{19}$$

The efficiency of pump is given by

$$\eta_f = d_1 + d_2 \left(\frac{Q}{N} \right) + d3 \left(\frac{Q}{N} \right)^2 \tag{20}$$

The power required by the pump to generate ΔH head at the speed N is given by

$$Power = \frac{\rho Q \Delta H_g}{\eta} \tag{21}$$

Temperature rise across the pump is given by

$$\Delta T = \frac{g \Delta H (1 - \eta_f)}{C_p \eta_f} \tag{22}$$

For LOX and LH2 pumps, HQN characteristics i.e. c_1,c_2,c_3,d_1,d_2,d_3 are obtained from cold flow tests.

8.2 Turbine

Specific enthalpy drop across the turbine is

$$\Delta h = C_p \Delta T \tag{23}$$

Efficiency of the turbine is given by

$$\eta_t = d_1 + d_2 \left(\frac{U_0}{C_0} \right) + d_3 \left(\frac{U_0}{C_0} \right)^2 \tag{24}$$

Power generated by the turbine is

$$Power_t = \dot{m} \Delta h \eta_t \tag{25}$$

8.3 Turbo-pump assembly

At every time step excess power available for the turbine is computed. Based on this the next instant speed is estimated using the following differential equation

$$\left(\frac{2\pi}{60} \right)^2 NI \frac{dN}{dt} = (\Delta Power) \tag{26}$$

In order to estimate the excess power, the power generated by the turbine and power consumed by both the pumps are needed. Flow and pressure budgets required for this are estimated using above mentioned mathematical models. During the steady state regime power generated by the turbine and the power consumed by the pumps are known. Hence using power balance

$$\dot{m} \Delta h \eta_t = \left[\frac{\rho Q \Delta H g}{\eta} \right]_{LH2pump} + \left[\frac{\rho Q \Delta H g}{\eta} \right]_{LOXpump} \tag{27}$$

9 Thrust and mixture ratio control

The thrust of the engine is regulated by controlling the LOX flow to the gas generator by means of a variable area flow control valve and using chamber pressure as feedback signal during ground tests. Using the feedback signal the thrust control electronics estimates the deviation from the requirements and command pulses required to nullify the deviation using the thrust control algorithm and actuates the thrust regulator. Mixture ratio is regulated in closed loop mode using a propellant flow control valve mounted in the engine LOX feed feed circuit.

The MRC system has a flow meter in the LOX and LH_2 propellant circuits and a LOX temperature sensor besides the regulator, electric drive and control electronics. Using

the feedback signals from flow meters & LOX temperature sensor real time mixture ratio, deviation in mixture ratio, and the command pulses required to correct the deviation in mixture ratio are estimated by MRC algorithm and the MRC regulator is actuated. The actuation of MRC regulator varies the hydraulic resistance in the engine LOX feed circuit to maintain the desired mixture ratio.

10 Feed lines

Pressure drop through the feed lines is estimated using the equation

$$\Delta p = \frac{4flV^2\rho}{2d} \tag{28}$$

11 Ignition peak and ignition time estimation

During the initial phase of start transient, while opening the propellant injection valves sequentially there will be propellant accumulation inside the combustion chamber. Ignition occurs, when the favorable ignition conditions (mixture ratio and temperature) are achieved in the chamber. Ignition peak is basically a strong function of this accumulated propellant inside the chamber. But in CUS engine before this pressure reaches the maximum value, two position valve in the thrust chamber LOX line acting as a metering valve opens fully and causes higher LOX flow. This flow dictates the maximum pressure spike inside the combustion chamber. For capturing these phenomena, a transient CFD simulation was carried out up to the ignition time and quasi steady state combustion modelling is carried out thereafter. Basic equations used for the modeling are given below.

The conservation of mass, momentum, energy and species conservation [4] are

$$\frac{\partial \rho}{\partial t} + \frac{\partial}{\partial x_j}(\rho U_j) = 0 \tag{29}$$

$$\frac{\partial}{\partial t}(\rho U_i) + \frac{\partial}{\partial x_j}(\rho U_i U_j) = -\frac{\partial P}{\partial x_i} - \frac{\partial \tau_{ij}}{\partial x_j} + \rho f_i \tag{30}$$

$$\frac{\partial}{\partial t}(\rho H) + \frac{\partial}{\partial x_j}(\rho U_j H) = \frac{\partial P}{\partial t} - \frac{\partial}{\partial x_j}(U_i \tau_{ij} + Q_j) + \rho U_i f_i. \tag{31}$$

$$\frac{\partial}{\partial t}(\rho C) + \frac{\partial}{\partial x_j}(\rho U_j C) = -\frac{\partial J_i}{\partial x_j} + R \tag{32}$$

where

$$\tau_{ij} = -\mu_b \delta_{ij} \frac{\partial U_l}{\partial x_l} - \mu\left(\frac{\partial U_i}{\partial x_j} + \frac{\partial U_j}{\partial x_i}\right);\ \mu_b = \frac{2}{3}\mu$$

$$H = E + \frac{P}{\rho} = e + \frac{1}{2}U_i U_i + \frac{P}{\rho} = h + \frac{1}{2}U_i U_i$$

Eddy dissipation model (EDM) is used for the simulation of combustion.

12 Results and discussion

The mathematical model along with transient CFD simulation is used for predicting the performance of CUS engine during the transient period. Ignition peak mainly depends on the accumulated propellants in the combustion chamber. Estimation of accumulated propellants inside the chamber using 1-dimensional equation is not possible. Hence accumulated quantity of propellants at the time of ignition is estimated using transient CFD simulation. Engine test sequence, mainly LOX injection valve opening time, has a crucial role on the ignition peak. Initially engine is working in the expander mode and engine parameters will build up during this time. The safe and smooth start of CUS engine requires a careful time sequence because it is a staged combustion cycle. As per the sequence H_2 injection valve opening command is at T0 + 0.5 s and LOX injection valve opening command is at T0 + 1.4 s. This time gap is mainly to establish H_2 in the coolant channel prior to the ignition of the engine for the safe thermal condition of the thrust chamber. If it is delayed further there is a possibility of hard start in the engine. Ground test of this engine is a challenging task due to the H_2 accumulation at the nozzle exit prior to the ignition of thrust chamber. For minimizing the H_2 accumulated quantity at the nozzle exit N_2 purging at the nozzle exit is used. Quantity required for this is finalized based on a series of simulations.

The model developed is used for the prediction of ignition characteristics of cryogenic engine flight acceptance hot test and a very good match is obtained in the test. Comparison of measured value and prediction value for the chamber pressure in flight engine acceptance test is given in Fig. 8. Turbo pump, thrust chamber and MRC characteristics are derived from cold flow tests. Engine build up during the transient phase mainly depends on the turbo pump efficiency at that operating regime which is derived from a series of hot tests and cold flow tests. The resistance of the thrust chamber coolant channel during transient phase is very complex due to two phase flow phenomenon in the channels. Ordinary heat transfer equations could not be used during this time due to complex two phase process in the coolant channels. Hence empirical relations derived from a number of hot tests are used in the model for the transient zone. The properties of propellants and combustion products are required for the simulation. Propellant

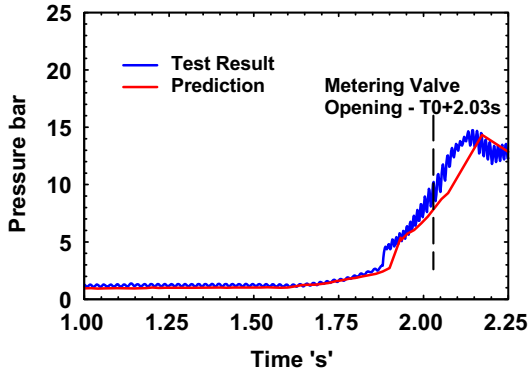

Fig. 8 Chamber pressure in flight engine acceptance test for GSLV-D5

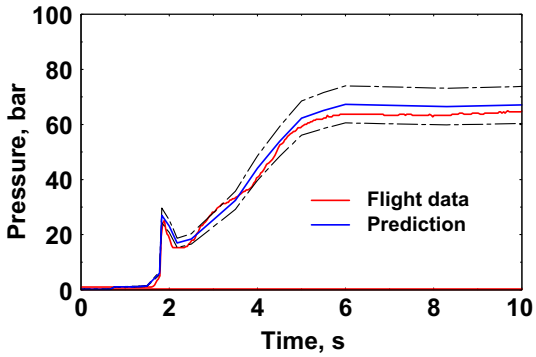

Fig. 9 LOX injection pressure

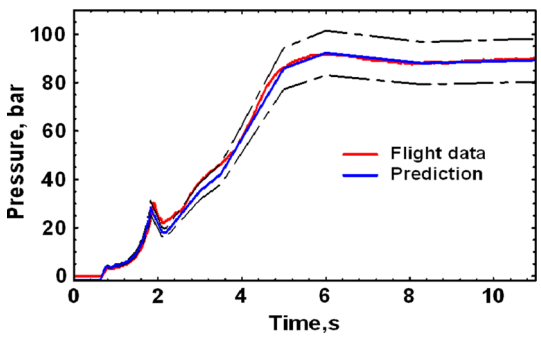

Fig. 10 Coolant channel outlet pressure

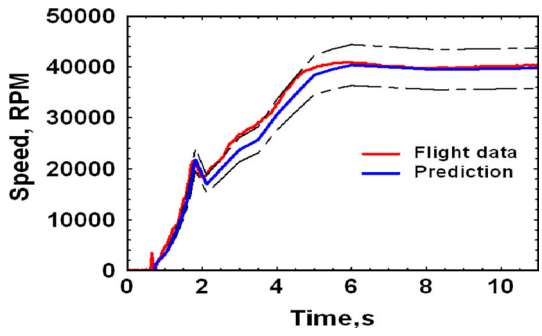

Fig. 11 Turbopump speed

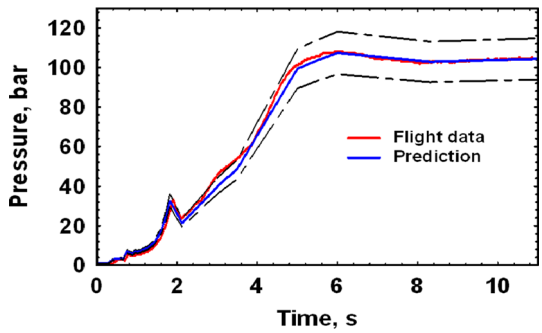

Fig. 12 H2 pump outlet pressure

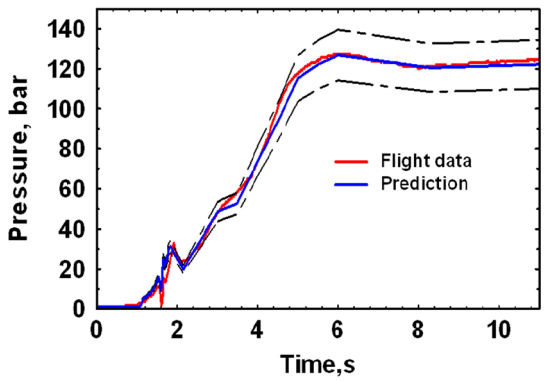

Fig. 13 LOX pump outlet pressure

properties are taken from "All Props" software and combustion product properties are estimated using CEC. Properties of combustion products are approximated by the curve fitting method. This validated model is used for the prediction of performance characteristics of CUS engine in GSLV D5 flight. Reasonably good match is obtained for all the major parameters of CUS engine in GSLV D5 and are given in Figs. 9, 10, 11, 12, 13. Figure 14 shows the estimated temperature distribution inside the chamber just after the ignition of main engine.

Comparison of flight data with prediction with respect to ignition time and parameters at the end of open loop are given in Table 1. Ignition time is predicted based on the favorable local mixture ratio and temperature. Temperature requirement for favorable ignition condition is above 800 K and the global mixture ratio requirement is 1.8–2 for main engine, 0.5–1.2 for Gas generator and 3–4 for steering engines. Variation in mixture ratio requirement is due to the different types of injector elements. Requirements are

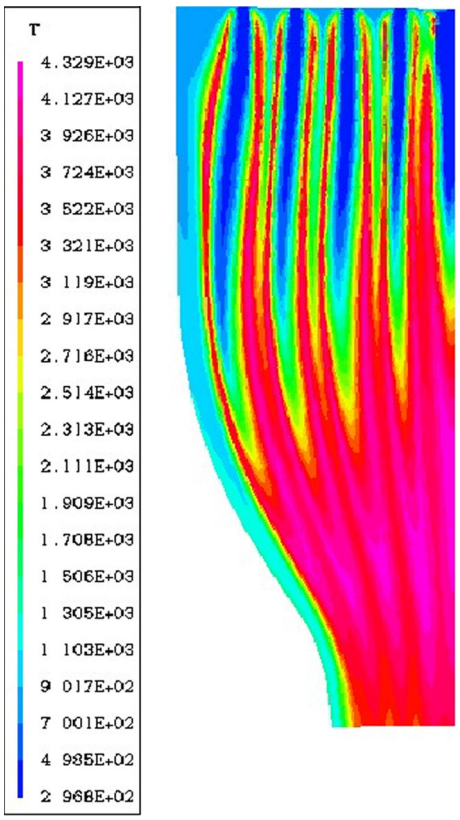

Fig. 14 Temp. distribution in ME just after ignition

Table 1 Ignition time

P parameter	Main engine	Steering engines	Gas generator
Expected ignition time (s)	1.75–1.81	1.1–1.45	2–2.3
Achieved ignition time (s)	1.8	Before ~1.5	2.05

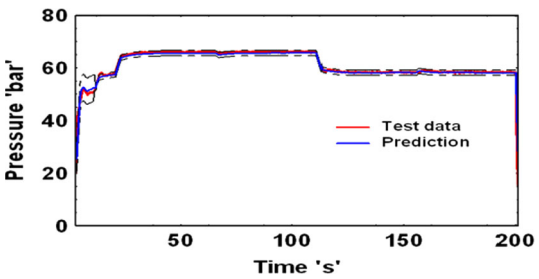

Fig. 15 Chamber pressure

derived based on the number hot tests results and simulations.

Comparison of major engine parameters with the prediction using the developed model is given in Figs. 15, 16, 17, 18. A very good match is obtained with the test results.

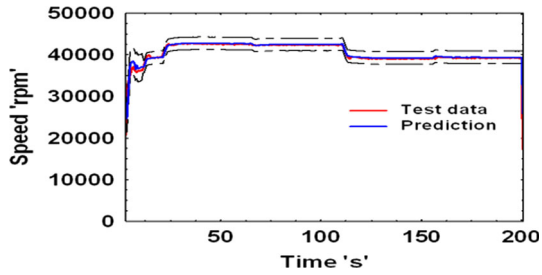

Fig. 16 Main turbo pump speed

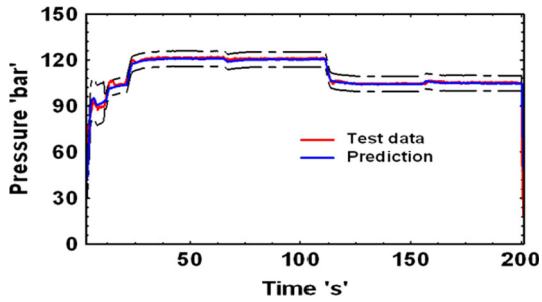

Fig. 17 LH2 pump outlet pressure

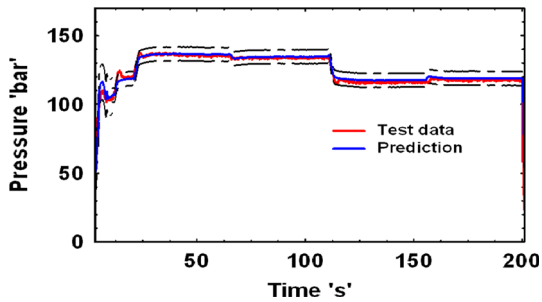

Fig. 18 LOX pump outlet pressure

13 Conclusion

A mathematical model is developed for the sequence finalisation, evaluation of subsystem performance under various test conditions and prediction of cryogenic engine performance during transient period and steady state regime. A method is evolved for the estimation of pressure peak at the time of ignition. Close match of the test results with the prediction during the transient and steady state period validates the developed code for the performance prediction of cryogenic engine.

References

1. Huzel, D.K., Huang, G.H.: Modern Engineering for Design of Liquid Propellant Rocket Engines. American Institute of Aeronautics and Astronautics, Washington D.C. (1992)

2. Sutton, G.P.: Rocket Propulsion Elements: An Introduction to the Engineering of Rockets. Wiley, New York (1992)
3. Gordon, S., MCBride, B.J.: Computer Program for calculation of Complex Chemical Equilibrium Compositions, Rocket Performance, Incident and Reflection shocks and Chapman-Jougent Detonations, NASA SP-273 (1971)
4. White, F.M.: Fluid Mechanics. McGraw-Hill Book Company, New York (1979)